Di- and Tetranuclear Dawson-Derived Sandwich Complexes: Synthesis, Spectroscopic Characterization, and Electrochemical Behavior

Laurent Ruhlmann,[a] Louis Nadjo,*[a] Jacqueline Canny,[b] Roland Contant,[b] and René Thouvenot*[b]

Keywords: Polyoxometalates / Sandwich complexes / Synthesis / NMR spectroscopy / Electrochemistry

The reaction of α-$[P_2W_{15}O_{56}]^{12-}$ with divalent cations M^{2+} leads to sandwich complexes of the formula $[M_4(H_2O)_2(P_2W_{15}O_{56})_2]^{16-}$ ($M_4P_4W_{30}$) where M = Mn^{II}, Co^{II}, Ni^{II}, Cu^{II}, Zn^{II}, or Cd^{II}. An Fe^{III} tetranuclear sandwich complex has also been obtained. Full details are reported concerning procedures by which the pure sandwich complexes can be obtained in good yield. A pure dinuclear trivalent Dawson-derived sandwich complex of the formula $[(H_2O)_2Na_2Fe^{III}_2(P_2W_{15}O_{56})_2]^{16-}$ has also been prepared as a water-soluble sodium salt. All the compounds have been characterized by IR spectroscopy, elemental analysis, and ^{31}P NMR spectrometry. The acid-base equilibria of the $M_4P_4W_{30}$ series have been studied. The electrochemical behavior of this series of sandwich complexes in aqueous solution has been investigated and systematic comparisons have been made. All these compounds exhibit successive reduction processes of the W atoms in a negative potential range, but in some cases the electrochemistry also involves redox reactions originating from the substituent transition metal (M), such as the reduction of Fe^{III} and Cu^{II} and the oxidation of Mn^{II}.

Introduction

The possibility of modifying the redox and chemical properties of heteropolyanions by replacing one or many elements renders them particularly attractive for catalytic and electrocatalytic applications.[1] For instance, a cluster such as $[P_2W_{18}O_{62}]^{6-}$ may be modified under hydrolytic conditions to give lacunary complexes containing one, three, or more vacant sites.[2] The action of metallic cations on the trivacant heteropoly ligand $[P_2W_{15}O_{56}]^{12-}$ (derived from the Dawson structure $[P_2W_{18}O_{62}]^{6-}$; Scheme 1) leads to metal-heteropolyanions that can be formulated as $[M_4(H_2O)_2(P_2W_{15}O_{56})_2]^{n-}$ (where M = Mn^{II}, Fe^{III}, Co^{II}, Ni^{II}, Cu^{II}, Zn^{II}, or Cd^{II}, and n = 16, except in the case of Fe^{III}, where n = 12). These constitute an extensive series of compounds in which a tetranuclear cluster $M_4O_{14}(H_2O)_2$ is encapsulated between two trivacant fragments.[3] Of the four metal atoms, two reside in a pseudooctahedral environment with one coordination site occupied by a labile water molecule, which can be replaced by other ligands.

This series of sandwich polyoxoanions with four d-electron transition metal cations appears quite promising as a potential class of catalysts because both the four central metal ions and, in principle, the heteroatoms in the trivacant polyoxoanions units can be varied considerably. Thus, they can be used in catalytic reactions as inorganic analogues of porphyrins with the advantage of being more robust and inert toward an oxidizing environment and more thermally stable than systems based on organic ligands.[4]

We report herein on a new route for the synthesis of a tetranuclear Co Dawson-derived sandwich complex as well as of a dinuclear Fe Dawson-derived sandwich complex[3i,3j] of the formula $[(H_2O)_2Na_2Fe_2(P_2W_{15}O_{56})_2]^{16-}$, which have been obtained when operating in acidic media.

We also present in the following a systematic spectroscopic investigation by ^{31}P NMR of the para- and diamagnetic sandwich complexes of the composition $[M_4(H_2O)_2(P_2W_{15}O_{56})_2]^{16-}$, as well as a study of their electrochemical behavior.

These sandwich complexes exhibit at least three consecutive processes involving oxo-tungsten based reduction in a negative potential range, but in some cases the electrochemistry also involves redox reactions originating from the substituent transition metal (M), such as the reduction of Fe^{III} and Cu^{II} and the oxidation of Mn^{II}.

Interestingly, for the compounds $[Fe_4(H_2O)_2P_4W_{30}O_{112}]^{12-}$ and $[(H_2O)_2Na_2Fe_2P_4W_{30}O_{112}]^{16-}$, the Fe-centered redox processes are fully reversible prior to reduction of the polyanions. Splitting of this wave is often seen.

[a] Laboratoire de Chimie Physique, Equipe d'Electrochimie et de Photoélectrochimie, UMR 8000, CNRS, Université Paris XI, Bâtiment 420,
91405 Orsay Cedex, France
E-mail: louis.nadjo@lcp.u-psud.fr
[b] Laboratoire de Chimie Inorganique et Matériaux Moléculaires, UMR 7071, CNRS, case courrier 42, Université Pierre et Marie Curie,
4, place Jussieu, 75252 Paris Cedex 05, France
E-mail: rth@ccr.jussieu.fr
Supporting information for this article is available on the WWW under http://www.eurjic.com or from the author.

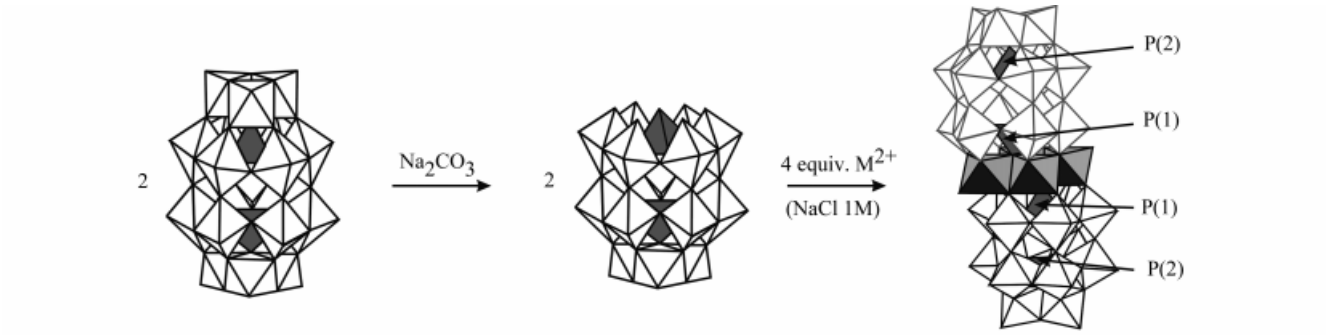

Scheme 1

Intriguingly, the Fe^{III}/Fe^{II} couples in $[(H_2O)_2Na_2Fe_2P_4W_{30}O_{112}]^{16-}$ ($Fe_2P_4W_{30}$) were found to be pH dependent; this is rather unusual for Fe-centered redox processes, for which the redox potential is usually almost pH-independent at low pH.[5] Assuming that $Fe_2P_4W_{30}$ has the molecular structure recently reported by Hill et al.,[3i,3j] with the two external sites of the sandwich structure occupied by Na^+ cations, the unusual pH dependence can be tentatively explained in terms of a stepwise exchange of the Na^+ cations by H^+ during the consecutive reduction of the two Fe^{III} centers.

To the best of our knowledge, such a complete investigation of Dawson sandwich species has not been published previously.

Results and Discussion

Synthesis

The first objective of this work was the large-scale, high-yielding preparation of very pure tetranuclear sandwich complexes of the composition $[M_4(H_2O)_2(P_2W_{15}O_{56})_2]^{16-}$. This polyanion consists of an oxo-aqua tetranuclear metal core, $M_4O_{14}(H_2O)_2$, sandwiched by two trivacant α-Dawson moieties, α-$[P_2W_{15}O_{56}]^{12-}$. The polyanion has C_{2h} symmetry (see Scheme 1).

Key factors in the strategy that led to the results described below included: (i) use of the pure lacunary precursor α-$[P_2W_{15}O_{56}]^{12-}$, (ii) extensive use of ^{31}P NMR spectroscopy to survey different conditions in optimizing the route to pure $[M_4(H_2O)_2(P_2W_{15}O_{56})_2]^{16-}$ products, (iii) careful control of the solution pH, and (iv) control of the stoichiometry of M^{n+} vs. α-$[P_2W_{15}O_{56}]^{12-}$ in order to obtain pure compounds.

The complexes were readily prepared in ca. 50−90% isolated yields and in high purity. The best preparation is similar to that cited in the literature for sandwich polytungstophosphate complexes $[M_4(H_2O)_2(P_2W_{15}O_{56})_2]^{16-}$, where M = Mn^{II}, Zn^{II}, or Cd^{II}.

However, to obtain pure $[Co_4(H_2O)_2(P_2W_{15}O_{56})_2]^{16-}$ it is necessary to operate in an acidic medium. Actually, as is evident from Figure 1, which shows the ^{31}P NMR spectra of $Co_4P_4W_{30}$ prepared by the literature method (neutral medium) and at ca. pH 3, the best preparation of pure $Co_4P_4W_{30}$ is undoubtedly achieved at pH 3. From the ^{31}P analysis, it appears that the preparation in neutral media, as described in the literature, invariably gives a mixture of several species, and that two different types of crystals, one green-brown and the other gray, are deposited from such solutions on crystallization. In contrast, the synthesis in acidic solution (ca. pH 3) leads exclusively to one major species as green-brown crystals with a purity of 95% (A in Figure 1).

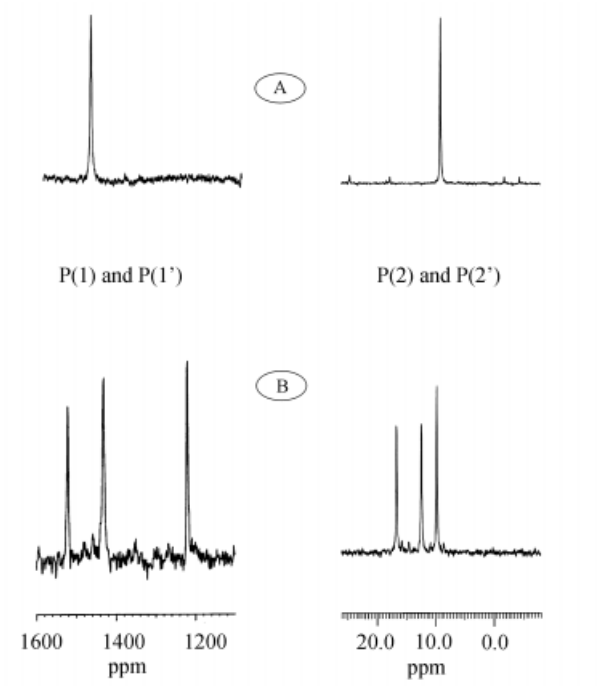

Figure 1. 121.5 MHz ^{31}P NMR spectra of $Co_4P_4W_{30}$ (0.02 M in 0.5 M aqueous LiCl): (A) sample prepared at pH 3; (B) sample prepared in neutral medium; left part: P(1) region; experimental conditions: spectral width 125 kHz; pulse width 2 μs (ca. 40° flip angle); 8K data points; acquisition time 33 ms; ca. 10K transients acquired without relaxation delay; line-broadening factor 40 Hz; right part: P(2) region; experimental conditions: spectral width 9 kHz; pulse width 2 μs (ca. 40° flip angle); 4K data points; acquisition time 0.23 s; ca. 1000 transients acquired without relaxation delay; line-broadening factor 4 Hz

The ^{31}P NMR spectrum of the mixture obtained following the synthesis in a neutral medium exhibits three "pairs"

Table 1. ^{31}P NMR data for α-P_2W_{15} and the sandwich species

Compound[a] δ≅[c]	P(1)[b] Δν[d]	δ[c]	P(2)[b] Δν[d]	
α-P_2W_{15}	+0.5	< 3	−13.8	< 3
$Mn_4P_4W_{30}$	[e]	130	−12.3	130
$Fe_2P_4W_{30}$	[e]	–	−11.2	220
$Fe_4P_4W_{30}$	+915	2500	−11.7	55
sym-$Co_4P_4W_{30}$	+1483	420	+9.9	20
sym-$Co_4P_4W_{30}$ [f]	+1459	420	+9.8	20
disym-$Co_4P_4W_{30}$ [f]	+1551	420	+16.7	20
	+1242	420	+12.3	20
sym-$Co_4P_4W_{30}$ [g]	+1473	1400	+8.8	25
disym-$Co_4P_4W_{30}$ [g]	+1590	1250	+16.7	30
	+1201	950	+10.1	40
$Ni_4P_4W_{30}$	+460	3400	−14.2	15
$Cu_4P_4W_{30}$	[e]	–	−16.2	60
$Zn_4P_4W_{30}$	−3.92	< 3	−13.95	< 3
$Cd_4P_4W_{30}$	−3.60	< 5	−14.36	< 3

[a] Unless otherwise noted, 0.02 M solution in 0.5 M LiCl. [b] P(1) and P(2) in the PW_6 and PW_9 subunits, respectively. [c] In ppm with respect to 85% H_3PO_4. [d] In Hz. [e] Not observed. [f] In a mixture as obtained from the synthesis medium (see text). [g] As for f, but in 0.1 M AcONa/AcOH buffer (pH 4.7).

of resonances (see Table 1 and B in Figure 1). The pair at δ = 1459 and 9.8 correspond to the two resonances of the pure $Co_4P_4W_{30}$ synthesized at pH 1 (see A in Figure 1). The four other signals will be considered below.

In more acidic solution (0.1 M AcONa/AcOH buffer), the ^{31}P NMR spectrum evolves by a concomitant decrease in the four resonances (at δ = 1590, 1201, 16.7, and 10.1). After one day, only the two peaks at δ = 1473 and 8.8 remain, which are characteristic of the pure $Co_4P_4W_{30}$ compound.

The chemical shift variations observed between neutral and acidic solutions can be attributed to deprotonation of the aqua ligands in neutral media (see below).

Because they disappear simultaneously at the expense of the $Co_4P_4W_{30}$ signals, the four resonances (at δ = 1590, 1201, 16.7, and 10.1) are most probably due to a single species, which contains four non-equivalent P atoms and should be structurally related to the symmetrical sandwich compound $Co_4P_4W_{30}$ (C_{2h}). Two unsymmetrical structural isomers of $Co_4P_4W_{30}$, both of C_s symmetry, can be considered, resulting from either (i) the formal π/3 rotation of the polar cap of one P_2W_{15} moiety, leading to a β-P_2W_{15} subunit (see Scheme 1) or (ii) the formal rotation of a whole α-P_2W_{15} subunit leading to both α-type and β-type junctions at the Co_4 tetrad.

Thus, in neutral solution, the synthesis of the Dawson sandwich species gives a mixture of symmetrical (δ = 1459 and 9.8) and unsymmetrical (δ = 1551, 1242, 16.7 and 12.3) complexes in relative proportions of 38 and 62% (by integration of the NMR resonances).

In acidic solution, only the symmetrical isomer is formed, which suggests that this isomer is the thermodynamic product obtained at pH 3 and that slow transformation occurs on decreasing the pH. Finke et al.[3b] described a similar behavior for $[Zn_4(H_2O)_2P_4W_{30}O_{112}]^{16-}$, where thermal isomerization was observed with the appearance of additional ^{31}P resonances. On the other hand, the temperature is not a factor in the present isomerization since the same temperature is used for the syntheses in acidic and neutral solutions. This result may suggest a control of the isomerization by the pH of the medium.

Di- and tetrairon sandwich polyoxoanions were prepared in 67% and 52% isolated yields, respectively, using essentially the same procedure. Actually, powdered α-$Na_{12}[P_2W_{15}O_{56}]$ dissolves readily at room temperature in an aqueous solution of iron(III) chloride (pH 3) without the formation of any insoluble intermediate. However, the optimal synthetic conditions were found when operating in more acidic media (pH 1) at high temperature (80 °C) and under vigorous stirring. With only one equivalent of α-P_2W_{15} added to the iron(III) solution, i.e. with one equivalent of Fe^{3+}, the diiron sandwich complex is obtained and can be isolated in high purity.

Conversely, with a stoichiometry of one equivalent of α-P_2W_{15} to two equivalents of Fe^{3+}, only the tetrairon sandwich compound is obtained as a pure species. This suggests an equilibrium between the di- and tetrairon sandwich polyoxoanions [Equation (1)]:

$$(H_2O)_2Na_2Fe^{III}_2(P_2W_{15}O_{56})_2^{16-} + 2\,Fe^{3+} \rightleftarrows Fe^{III}_4(H_2O)_2(P_2W_{15}O_{56})_2^{12-} + 2\,Na^+ \quad (1)$$

Accordingly, the "unsaturated" diiron species must be formed first and exists predominantly at low Fe^{3+}/α-P_2W_{15} ratios. It is converted to the "saturated" tetrairon species in the presence of an excess of iron.

IR Characterization

The IR spectrum of $Zn_4P_4W_{30}$ is shown Figure 2 and is compared with those of the parent anions α-P_2W_{15} and α-P_2W_{18}.

Apart from the W−O bands, which appear at low wavenumbers (< 1000 cm^{-1}), the IR spectra of phosphorus-centered polyoxotungstates are characterized by well-separated P−O stretching vibrations between 1200 and 1000 cm^{-1}.[6]

According to the local symmetry of the PO_4 group, the triply-degenerate mode F_2 (for T_d symmetry) may split into two or three absorption bands for C_{3v} or C_s symmetry, respectively; the splitting depends on the deviation from ideal symmetry. Hence, for the lacunary anions $[PMo_{11}]$ and $[PW_{11}]$, and for the substituted metallophosphates $[PMMo_{11}]$ and $[PMW_{11}]$ (M = first row transition metal), it was shown that the splitting Δν decreases when the metal M interacts more strongly with the oxygen atom of the PO_4 tetrahedron.[7] For lacunary or substituted unsymmetrical Dawson species, the situation is more intricate due to the overlap of vibrational absorption bands arising from two different PO_4 tetrahedra; in favorable cases, however, it is possible to discriminate between the bands arising from the unperturbed subunit PW_9 and those arising from the PW_xM_y moiety.[8] For example, α-P_2W_{15}, like α-P_2W_{18}, ex-

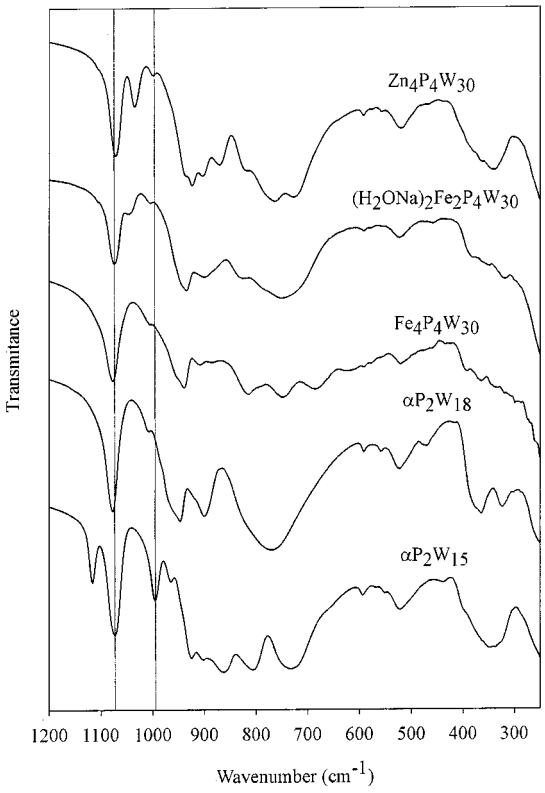

Figure 2. Comparison of the IR spectra (KBr) of the hydrated sandwich compounds $Zn_4P_4W_{30}$, $Fe_2P_4W_{30}$, $Fe_4P_4W_{30}$, and of their precursors

hibits two bands at around 1080 and 1010 cm^{-1} (assigned to PW_9), as well as an additional band at high wavenumbers (1131 cm^{-1}), which can be attributed to the PW_6 subunit. The corresponding vibrational mode may be described as a stretching of the $P-O_{ter}$ bond along the ternary axis (A_1-type in the C_{3v} point group) and the relatively high frequency is related to the large force constant of this bond, which has some P=O double bond character. This band is not observed for the sandwich compounds $M_4P_4W_{30}$, in agreement with the fact that the oxygen atom has contracted bonds with some M atoms, which results in a decrease of the k_{P-O} force constant. Actually, it appears that the band associated with the PW_6 subunit is correspondingly shifted to low wavenumbers and all of the tetrametallic sandwich compounds, except for $Fe_4P_4W_{30}$, exhibit a band at about 1055 cm^{-1}. The IR spectra of the Mn, Co, Ni, Cu, Zn, and Cd derivatives are nearly identical, which indicates a structural similarity throughout the whole $M_4P_4W_{30}$ series. Finally, we note that terminal W−O and bridging W−O−W stretching bands are located in the range 970−700 cm^{-1}, at lower wavenumbers than for the parent saturated α-P_2W_{18} anion.

Let us return to the case of the iron compounds: in the phosphate stretching region, the IR spectrum of $Fe_4P_4W_{30}$ exhibits the same pattern as that of P_2W_{18}, and no band is present at around 1060 cm^{-1} (Figure 2). This indicates that both PO_4 groups in the PW_6 and PW_9 moieties are becoming nearly equivalent, most probably because of the stronger M−O interaction exerted by the trivalent Fe^{3+} ions as compared with those of the divalent Mn^{2+}, Co^{2+}, Ni^{2+}, Cu^{2+}, Zn^{2+}, and Cd^{2+} cations. For $[Fe_2P_4W_{30}]$, however, only two iron atoms may interact with the oxygen atom of the phosphate, which is insufficient to restore the equivalence of the two PO_4 groups belonging to the two subunits; this accounts for the presence of the small absorption band at almost the same wavenumber as seen for the $M_4^{II}P_4W_{30}$ species.

^{31}P NMR Characterization

^{31}P NMR spectroscopy is particularly well-suited for checking the purities of polyoxometallate species and for characterizing the nature of the substituting elements. The ^{31}P NMR spectroscopic data for the sandwich complexes $[M_4(H_2O)_2(P_2W_{15}O_{56})_2]^{16-}$ (M = Mn^{2+}, Co^{2+}, Ni^{2+}, Cu^{2+}, Zn^{2+}, and Cd^{2+}), $[Fe_4^{III}(H_2O)_2(P_2W_{15}O_{56})_2]^{12-}$ and $[(H_2O)_2Na_2Fe_2^{III}(P_2W_{15}O_{56})_2]^{16-}$ ($Fe_2P_4W_{30}$), and their parent compounds are reported in Table 1. The ^{31}P NMR spectra of the diamagnetic species $Cd_4P_4W_{30}$ and $Zn_4P_4W_{30}$ show two lines, consistent with the presence of a single isomer (Figure 3); the most shielded line, at about $\delta = -14$, is assigned to P(2) of the PW_9 unit. The deshielded line, at about $\delta = -4$, corresponds to P(1) in the PW_6M_3 unit; its integrated intensity appears smaller than that of P(2) because of a slow relaxation rate (large T_1).

In comparison with the diamagnetic complexes, the spectra of the paramagnetic compounds are characterized by broad signals and large frequency shifts. For paramagnetic species, the signals can be assigned according to the following rule: the most broadened and shifted resonances correspond to the atoms nearest to the paramagnetic centers. Then, for each sandwich compound, the sharper line, with a chemical shift close to those seen for diamagnetic metallophosphates (between $\delta = +20$ and $\delta = -20$) is assigned to P(2), the P atom furthest from the M^{n+} ions. The P(1) atom, which is very close to the paramagnetic elements, is responsible for the broad and strongly deshielded resonances. For $Ni_4P_4W_{30}$, the broadening of the P(1) signal makes the line difficult to discern accurately from base-line artifacts. Figures 1, 3, and 4 show typical ^{31}P NMR spectra of $M_4P_4W_{30}$ and $Fe_2P_4W_{30}$ Dawson sandwich complexes.

For the series of sandwich complexes, the observed line widths, $\Delta\nu_{1/2}$, for the P(1) resonance are as follows: for the diamagnetic Zn^{2+} and Cd^{2+} complexes the signal is very narrow ($\Delta\nu_{1/2} < 5$ Hz); for Co^{2+} complexes it is relatively narrow ($\Delta\nu_{1/2} = 420$ Hz), while for tetrametallic Fe^{3+} and Ni^{2+} complexes it is very broad ($\Delta\nu_{1/2} = 2500$ Hz and 3400 Hz, respectively). In the case of Cu^{2+} and Mn^{2+}, as well as for the diiron species, the signals from P(1) are probably too broad to be observed. As a consequence, the spectra of these complexes feature only one resonance, corresponding to the P(2) atom.

The same trend in line width is also observed for the P(2) signal (the P atom furthest from the M^{n+} ions). The line width $\Delta\nu_{1/2}$ for P(2) varies as follows: for the diamagnetic Zn^{2+} and Cd^{2+} complexes the signal is very narrow ($\Delta\nu_{1/2} < 3$ Hz), it remains relatively narrow for Co^{2+} and Ni^{2+} (in

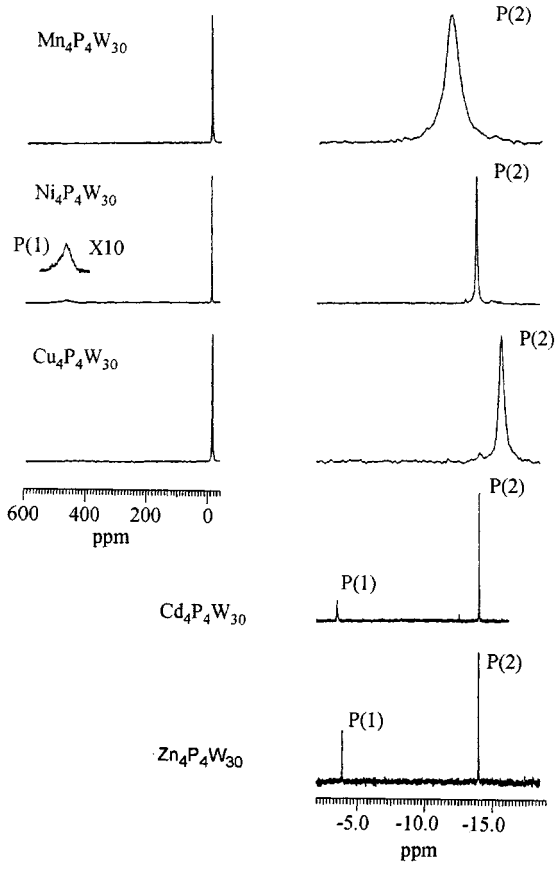

Figure 3. 121.5 MHz ^{31}P NMR spectra of various $M_4P_4W_{30}$ species (0.02 M in 0.5 M aqueous LiCl); experimental conditions for the left part: spectral width 166 kHz; pulse width 2 μs (ca. 40° flip angle); 4K data points; acquisition time 13 ms; ca. 70K transients acquired without relaxation delay; line-broadening factor 80 Hz; experimental conditions for the right part: $Cd_4P_4W_{30}$ and $Zn_4P_4W_{30}$: spectral width 2.5 kHz; 8K data points; acquisition time 1.6 s; ca. 300 transients acquired without relaxation delay; line-broadening factor 0.6 Hz; $Mn_4P_4W_{30}$, $Ni_4P_4W_{30}$, and $Cu_4P_4W_{30}$: spectral width 6 kHz; 4K data points; acquisition time 0.3 s; ca. 2000 transients acquired without relaxation delay; line-broadening factor 20 Hz (Mn), 3 Hz (Ni), and 10 Hz (Cu)

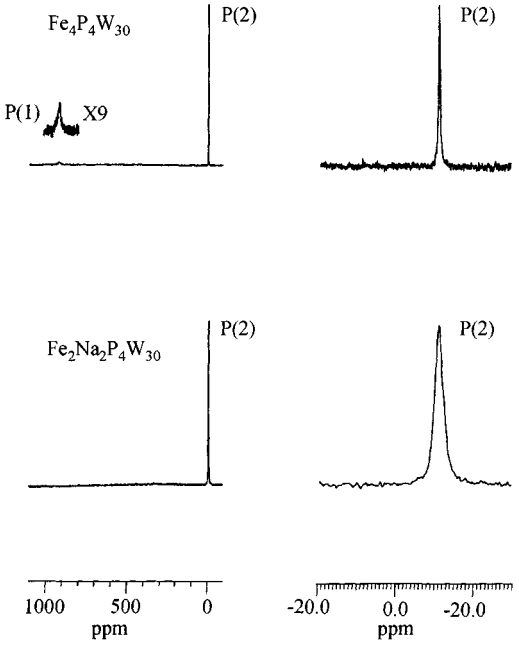

Figure 4. 121.5 MHz ^{31}P NMR spectra of $Fe_4P_4W_{30}$ and $Na_2Fe_2P_4W_{30}$ (0.02 M in 0.5 M aqueous LiCl); experimental conditions for the left part: spectral width 166 kHz; pulse width 2 μs (ca. 40° flip angle); 4K data points; acquisition time 13 ms; ca. 70K transients acquired without relaxation delay; line-broadening factor 80 Hz; experimental conditions for the right part: spectral width 10 kHz; 4K data points; acquisition time 0.2 s; ca. 3000 transients acquired without relaxation delay; line-broadening factor 10 Hz ($Fe_4P_4W_{30}$) and 10 Hz ($Na_2Fe_2P_4W_{30}$)

the range 15−20 Hz), but is markedly broadened for Mn^{2+} ($\Delta\nu_{1/2}$ = 130 Hz) and for the diiron species ($\Delta\nu_{1/2}$ = 220 Hz). For Cu^{2+} and for the tetrairon species, the signal is of intermediate width ($\Delta\nu_{1/2}$ = 60 Hz and 55 Hz, respectively).

A similar variation in ^{31}P line width has previously been observed by Baker et al. for Keggin and Dawson monosubstituted polytungstates.[9] Baker noted that complexes containing paramagnetic ions with orbitally nondegenerate ground states (i.e. Mn^{2+}, $^6A_{1g}$) are those giving very broad ^{31}P signals. Orbitally nondegenerate states have long electronic relaxation times, which lead to very fast nuclear relaxation of the nearby nuclei (short T_1 and T_2). Therefore, in accordance with the relationship $\Delta\nu_{1/2} = 1/\pi T_2$, the NMR resonances are very broad. On the contrary, for orbitally degenerate ground states, such as Co^{2+} ($^4T_{1g}$), the fast electronic relaxation rate leads to relatively slow nuclear relaxation, which explains the relatively narrow NMR lines.[9]

pK_a Determination

In the sandwich compounds, the sixth coordination position of the external metal atoms is occupied by a labile water molecule. According to the pH, this aqua ligand can be easily deprotonated, successively giving the hydroxo-aqua and the dihydroxo forms [Equations (2) and (3)].

$$M_4^{II}(H_2O)_2P_4W_{30}O_{112}^{16-} + H_2O \rightleftarrows M_4^{II}(H_2O)(OH)P_4W_{30}O_{112}^{17-} + H_3O^+ \quad pKa_1 \tag{2}$$

$$M_4^{II}(H_2O)(OH)\,P_4W_{30}O_{112}^{17-} + H_2O \rightleftarrows M_4^{II}(OH)_2P_4W_{30}O_{112}^{18-} + H_3O^+ \quad pKa_2 \tag{3}$$

The dihydroxo forms of the M^{II} sandwich complexes were obtained directly from their syntheses in neutral solutions, except in the case of the Co^{II} species. For the titration, the hydroxo-aqua form of $Co_4P_4W_{30}$, as obtained from the synthesis at ca. pH 3, was initially converted to its dihydroxo form by adding a stoichiometric amount of NaOH.

Acidification curves of the dihydroxo complexes do not depend on the concentration and show the successive protonation of the two hydroxo groups. Actually, the diacid character of the sandwich complex could be confirmed by a pH jump in the presence of two equivalents of HNO_3.

The titration curves are characteristic of diacid behavior where pK_{a1} and pK_{a2} are close.

K_{a1} and K_{a2} were calculated from experimental points using the following relationship (A):

$$[H_3O^+] = \frac{-(1-x)Ka_1 + \sqrt{Ka_1^2(1-x)2 + 4xKa_1Ka_2(2-x)}}{2(2-x)} \quad (A)$$

where x is the number of mol of HNO_3 per mol of complex. The values of pK_{a1} and pK_{a2} are reported in Table 2.

Table 2. Acidity constants for the sandwich species $M_4P_4W_{30}$ and $Fe_2P_4W_{30}$

Compound	pK_{a1}	pK_{a2}
$Mn_4P_4W_{30}$	3.5 ± 0.1	5.3 ± 0.1
$Fe_4P_4W_{30}$	3.6 ± 0.1	5.6 ± 0.1
$Fe_2P_4W_{30}$	3.6 ± 0.1	5.6 ± 0.1
$Co_4P_4W_{30}$	3.5 ± 0.1	5.3 ± 0.1
$Ni_4P_4W_{30}$	—[a]	—[a]
$Cu_4P_4W_{30}$	3.2 ± 0.1	5.0 ± 0.1
$Zn_4P_4W_{30}$	3.2 ± 0.1	5.2 ± 0.1
$Cd_4P_4W_{30}$	3.6 ± 0.1	5.4 ± 0.1

[a] Degradation occurred during the titration.

In the case of iron(III) complexes, as their syntheses were conducted in acidic solutions, they were obtained as diaqua species. Therefore, their acidity constants were determined from the titration of their diaqua forms with NaOH. This corresponds to the successive deprotonation of the two aqua ligands. pK_{a1} and pK_{a2} were obtained by analysis of the basification curves using the following relationship (B):

$$[H_3O^+] = \frac{(1-x)Ka_1 + \sqrt{Ka_1^2(1-x)2 + 4xKa_1Ka_2(2-x)}}{2x} \quad (B)$$

where x is the number of mol of NaOH per mol of complex.

Electrochemistry

General Electrochemical Behavior

The electrochemical behavior of sandwich complexes of the composition $[M_4(H_2O)_2(P_2W_{15}O_{56})_2]^{16-}$ ($M_4P_4W_{30}$) was mainly studied in aqueous solutions by cyclic voltammetry (CV). $M_4P_4W_{30}$ complexes are stable in aqueous media in the pH range 1−6 (with the exception of the $Ni_4P_4W_{30}$ sandwich, for which slow degradation was observed during the titration).

Beyond this pH range, the complexes become unstable due to hydrolytic decomposition.

These sandwich complexes exhibit at least three successive processes involving W in a negative potential range. Some of them also undergo redox reactions originating from the substituent transition metal (M), such as the reduction of Fe^{III} and Cu^{II} at less negative potentials and the oxidation of Mn^{II} at a more positive potential. In general, the reduction of heteropolyanions is accompanied by protonation at low pH, and hence the pH of the solution has a great effect on the electrochemical behavior of the sandwich. For the three couples corresponding to oxo W-based reduction, the cathodic peak currents are almost proportional to the square root of the scan rate up to 500 mV s^{-1}, which indicates that the electrode reaction of $M_4P_4W_{30}$ is diffusion controlled.

All electrochemical data acquired at pH 2.52 are gathered in Table 3 and typical cyclic voltammograms are presented in Figures 5−9.

$M_4P_4W_{30}$ Complexes with Electrochemically Silent Heterometallic Ions, M = Co^{2+}, Ni^{2+}, Zn^{2+}, Cd^{2+}

The electrochemical behavior of all $M_4P_4W_{30}$ complexes with M = Co^{2+}, Ni^{2+}, Zn^{2+}, or Cd^{2+} is very similar. Therefore, only the characteristics of the Co compound will be described in detail. CVs of $Co_4P_4W_{30}$ in aqueous solutions at pH 2.52 are presented in Figure 5. $Co_4P_4W_{30}$ is stable in aqueous solution in the pH range 1−6. At pH > 6, the cyclic voltammogram becomes ill-defined and the peak current is much smaller; such an observation has previously been reported by Dong et al. in relation to Keggin-type polyoxometallates;[10] this behavior may be due to a repulsion of the 18^- charge of $Co_4P_4W_{30}$ at the glassy carbon electrode surface.

In the pH range 1−6, three well-defined redox waves originating from the oxo-tungsten framework are seen between −0.30 and −0.95 V. These three redox couples with equal heights all relate to four-electron reaction processes, as determined by coulometry. At more acidic pH (in the range 1−3), the redox potentials of the three four-electron waves become more negative; the first and the last four-electron waves for M = Co^{2+} or Ni^{2+} split into two two-electron waves (see B in Figure 5). Thus, in the pH range 1−3, the formal potentials of all three pairs of waves are pH dependent; the slopes of plots of the formal potentials vs. pH lie in the range 80−95 mV per pH unit, which indicates the addition of two or four H^+ ions to the reduced form of each redox couple. Above pH 3, the formal potentials for the two first redox couples are influenced by pH to a lesser degree, and they are shifted only slightly to more negative values with increasing pH. On the contrary, the formal potential of the third redox process is shifted slightly in the positive direction at pH > 3. These results show that H^+ does not participate in the redox reaction at pH > 3.

In addition, a fourth reduction wave is observed in the more negative range, between −1.00 and −1.20 V. It is an irreversible multi-electron wave that overlaps with the hydrogen evolution, and is not shown in the figure. In the more positive potential range between +1.60 and −0.30 V, however, no redox waves are observed, suggesting that the four sandwich complexes with Co, Ni, Zn, and Cd divalent

Table 3. Electrochemical data for the sandwich species $M_4P_4W_{30}$ and $Fe_2P_4W_{30}$

Compound[a]	W(1)	W(2)	W(3)	$Fe^{III/II}$	$Mn^{IV/II}$	$Mn^{IV/III}$	$Mn^{III/II}$	Cu(ox)	Cu(red)
$Mn_4P_4W_{30}$	−0.404 (4e)	−0.533 (4e)	−0.733 (4e)	−	1.000 (8e)	0.800 (4e)	0.004 (4e)	−	−
$Fe_4P_4W_{30}$	−0.352 (2e)	−0.517 (4e)	−0.735 (4e)	0.187 (1e)	−	−	−	−	−
	−0.403 (2e)			0.110 (1e)					
				−0.028 (2e)					
$Fe_2P_4W_{30}$	−0.350 (2e)	−0.530 (4e)	−0.755 (4e)	−0.060 (1e)	−	−	−	−	−
	−0.407 (2e)			−0.164 (1e)					
$Co_4P_4W_{30}$	−0.354 (2e)	−0.534 (4e)	−0.788 (2e)	−	−	−	−	−	−
	−0.416 (2e)		−0.837 (2e)						
$Ni_4P_4W_{30}$	−0.366 (4e)	−0.472 (4e)	−0.755 (4e)	−	−	−	−	−	−
$Cu_4P_4W_{30}$	−0.295[b]	−	−	−	−	−	−	$E_{pa} = -0.004$	$E_{pc} = -0.150$
	−0.353[b]								
$Zn_4P_4W_{30}$	−0.358 (4e)	−0.583 (4e)	−0.748 (4e)	−	−	−	−	−	−
$Cd_4P_4W_{30}$	−0.400 (4e)	−0.703 (4e)	−0.779 (4e)	−	−	−	−	−	−
αP_2W_{15}	−0.590 (4e)[c]	−0.812 (2e)[c]							
	−0.52 (4e)[d]	−0.78 (2e)[d]							

[a] All redox potentials $E^{\circ\prime}$, approximated by $(E_{pa} + E_{pc})/2$ for the reversible steps, are given in V vs. SCE as obtained from cyclic voltammetry ($v = 20\ mV\ s^{-1}$) in 0.5 M $Na_2SO_4 + H_2SO_4$ (pH 2.52). [b] Irreversible. [c] In 0.1 M acetic acid/lithium acetate buffer, GC electrode. [d] In 1 M acetic acid/lithium acetate buffer, Hg electrode.

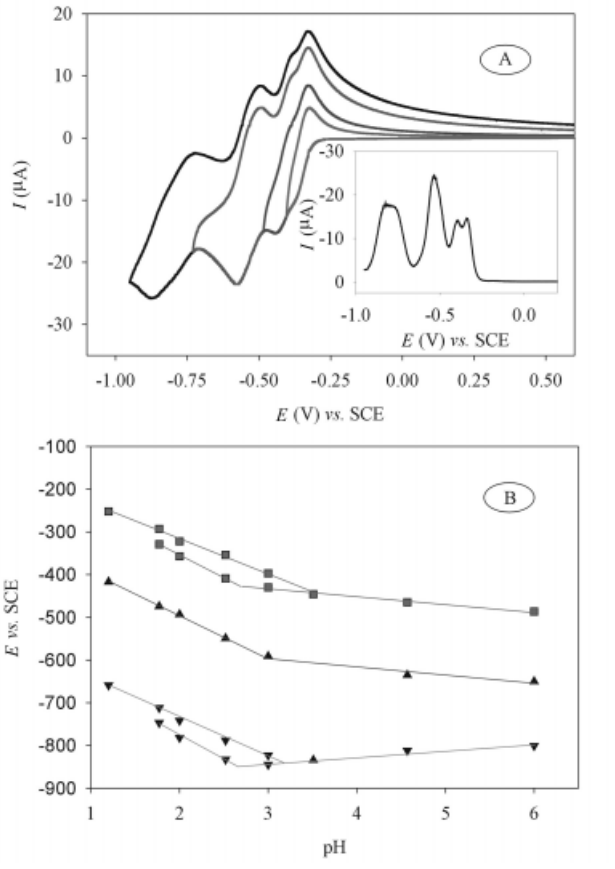

Figure 5. (A) Cyclic voltammograms of 1 mM $Co_4P_4W_{30}$ in 0.5 M $Na_2SO_4 + H_2SO_4$ at pH 2.52 with different negative potential limits: −0.30 V, −0.45 V, −0.70 V, and −0.90 V; scan rate 20 mV s^{-1}; inset: differential pulse voltammetry; scan rate 25 mV s^{-1}; (B) half-wave potential vs. pH plots for the first (■), second (▲), and third tungsten redox couples (▼)

transition metal cations are not electroactive under our experimental conditions.

$Fe_2P_4W_{30}$ and $M_4P_4W_{30}$ Complexes with Electroactive Substituent Metals, M = Mn^{2+}, Cu^{2+}, Fe^{3+}

$[Mn_4(H_2O)_2(P_2W_{15}O_{56})_2]^{16-}$ ($Mn_4P_4W_{30}$): CVs of the compound ($Mn_4P_4W_{30}$) at pH 2.52 are shown in Figure 6.

Three couples of oxo-tungsten based reduction processes can be seen at negative potentials in Figure 6, close to those of other $M_4P_4W_{30}$ species (M = Co, Ni, Zn, and Cd). The fourth reduction wave is a multi-electron wave that overlaps with the hydrogen evolution and is not shown in the figure. A new pair of redox process is observed at positive potentials of 1.00 V for oxidation and 0.80 V for reduction, which must correspond to the Mn-centered reaction (see B in Figure 6).[11] Controlled-potential electrolysis oxidation at +1.20 V (pH 2.52) resulted in the passage of 8.2 electrons per molecular anion, whereas subsequent reduction at +0.60 V consumes 4.2 electrons. These results show that the Mn-centered anodic peak corresponds to an eight-electron process, which suggests simultaneous oxidation of the four Mn^{II} heterometals to Mn^{IV} at +1.00 V and reduction of Mn^{IV} to Mn^{III} at 0.80 V. When the pH is increased, the peak potentials of both W- and Mn-centered redox waves of $Mn_4P_4W_{30}$ shift in the negative direction, indicating that they are all accompanied by protonation. Additionally, a new cathodic peak appears at −0.08 V.

Figure 6 (A) shows that the appearance of the new cathodic peak is closely related to the Mn oxidation state. This new cathodic peak appears in the CVs only after the Mn-centered redox wave. It can be seen that as the preconditioning time at +1.00 V increases, the new cathodic peak at −0.08 V grows gradually, the peak current of the first Mn-centered reduction at 0.80 V increases simultaneously, while the W-based peak currents remain unchanged.

Similar results have also been obtained for α_2-MnP_2W_{17} and $ZnW_{11}Mn$ polyanions.[10] The present results suggest the oxidation of Mn^{II} to Mn^{IV} at ca. 1.00 V followed by the

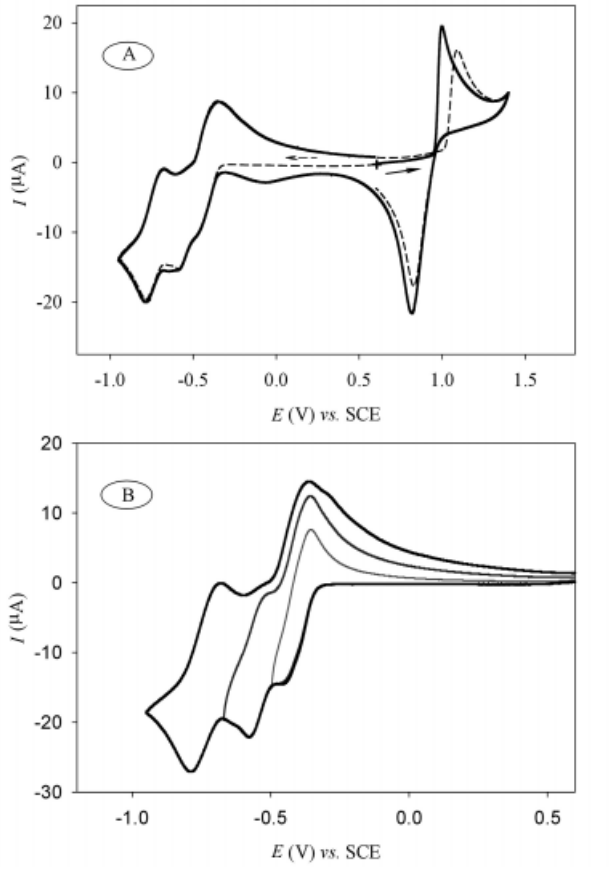

Figure 6. (A) Cyclic voltammograms of 1 mM $Mn_4P_4W_{30}$ in 0.5 M Na_2SO_4 + H_2SO_4 at pH 2.52; scan rate 10 mV s^{-1}; the arrows indicate the sweep direction; (B) cyclic voltammograms of 1 mM $Mn_4P_4W_{30}$ in 0.5 M Na_2SO_4 + H_2SO_4 at pH 2.52 with different negative potential limits: −0.45 V, −0.65 V, and −0.95 V; scan rate 10 mV s^{-1}

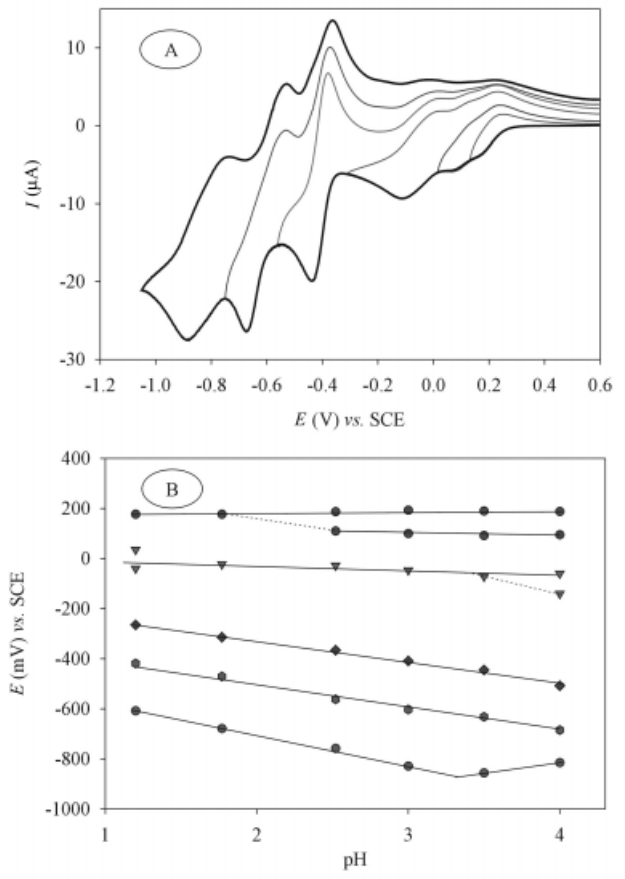

Figure 7. (A) Cyclic voltammograms of 1 mM $Fe_4P_4W_{30}$ in 0.5 M Na_2SO_4 + H_2SO_4 at pH 2.52 with different negative potential limits: −0.13 V, −0.30 V, −0.39 V, −0.47 V, −0.69 V, and −0.95 V; scan rate 20 mV s^{-1}; inset: differential pulse voltammetry; scan rate 25 mV s^{-1}; (B) half-wave potential vs. pH plots for the $Fe^{III/II}$ redox couples (● and ▼) and the first (◆), second (■), and third tungsten redox couples (●)

reduction of Mn^{IV} to Mn^{III} at ca. 0.80 V and reduction of Mn^{III} to Mn^{II} at ca. −0.08 V on the reverse scan.

$[Fe_4^{III}(H_2O)_2(P_2W_{15}O_{56})_2]^{12-}$ ($Fe_4P_4W_{30}$): This species is stable in aqueous solution in the pH range 0.24−6.0, but at pH > 4 the cyclic voltammogram becomes ill-defined and the peak current is much smaller. No redox process is seen between 0.30 and 1.60 V; on the cathodic part, three or (depending on the pH) four $Fe^{III/II}$ reduction waves and three W reduction waves are observed. The positions of these three tungsten oxo reduction waves were studied as a function of pH; the formal potentials were found to shift by 87−95 mV per pH unit, which indicates the addition of one or two protons to the reduced forms of each redox couple.

In contrast, the three Fe-centered waves are almost pH independent. These results show that H^+ does not participate in the Fe-centered redox reaction in the pH range 0.24−6.00. At pH 2.52, two reversible one-electron and one reversible two-electron waves appear (Figure 7) with $E^{\circ\prime}$ values of +0.187 V, +0.110 V, and −0.028 V (ΔE_p = 74, 68, and 112 mV, respectively). Controlled potential electrolysis at −0.20 V in a medium at pH 2.52 and under continuous argon bubbling indicated the involvement of 4.10 electrons per molecule.

The reduction processes of $Fe_4P_4W_{30}$ can be represented as follows [Equations (4)−(6)].

$$[Fe_4^{III}(H_2O)_2(P_2W_{15}O_{56})_2]^{12-} + e^- \leftrightharpoons [Fe_3^{III}Fe^{II}(H_2O)_2(P_2W_{15}O_{56})_2]^{13-} \quad (4)$$

$$[Fe_3^{III}Fe^{II}(H_2O)_2(P_2W_{15}O_{56})_2]^{13-} + e^- \leftrightharpoons [Fe_2^{III}Fe_2^{II}(H_2O)_2(P_2W_{15}O_{56})_2]^{14-} \quad (5)$$

$$[Fe_2^{III}Fe_2^{II}(H_2O)_2(P_2W_{15}O_{56})_2]^{14-} + 2e^- \leftrightharpoons [Fe_4^{II}(H_2O)_2(P_2W_{15}O_{56})_2]^{16-} \text{ (at pH} < 3.5) \quad (6)$$

$[(H_2O)_2Na_2Fe_2(P_2W_{15}O_{56})_2]^{16-}$ ($Fe_2P_4W_{30}$): This species is stable in aqueous solution in the pH range 0.24−7.00. As shown in Figure 8, at pH 2.52 it also exhibits three four-electron waves at negative potentials close to those of $M_4P_4W_{30}$ (M = Co, Ni, Zn, and Cd). The positions of these three tungsten oxo reduction waves were found to be pH dependent. The slopes of plots of the formal potential vs. pH vary in the range 55−80 mV per pH unit. This is indicative of the addition of four protons to the reduced forms of each redox couple.

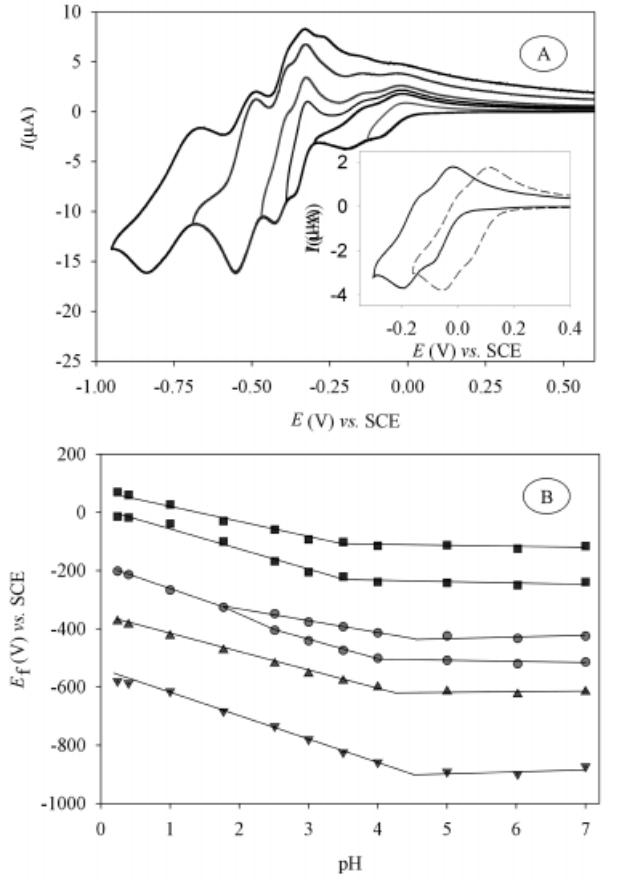

Figure 8. (A) Cyclic voltammograms of 1 mM $Na_2Fe_2P_4W_{30}$ in 0.5 M Na_2SO_4 + H_2SO_4 at pH 2.52 with different negative potential limits: −0.13 V, −0.30 V, −0.39 V, −0.47 V, −0.69 V, and −0.95 V; scan rate 20 mV s^{-1}; (B) half-wave potential vs. pH plots for the $Fe^{III/II}$ redox couples (■), and the first (●), second (▲), and third tungsten redox couples (▼); inset: the voltammograms are restricted to the first waves of the cathodic patterns, which corresponds to the $Fe^{III/II}$ couples; solid line: pH 2.52; dotted line: pH 0.24

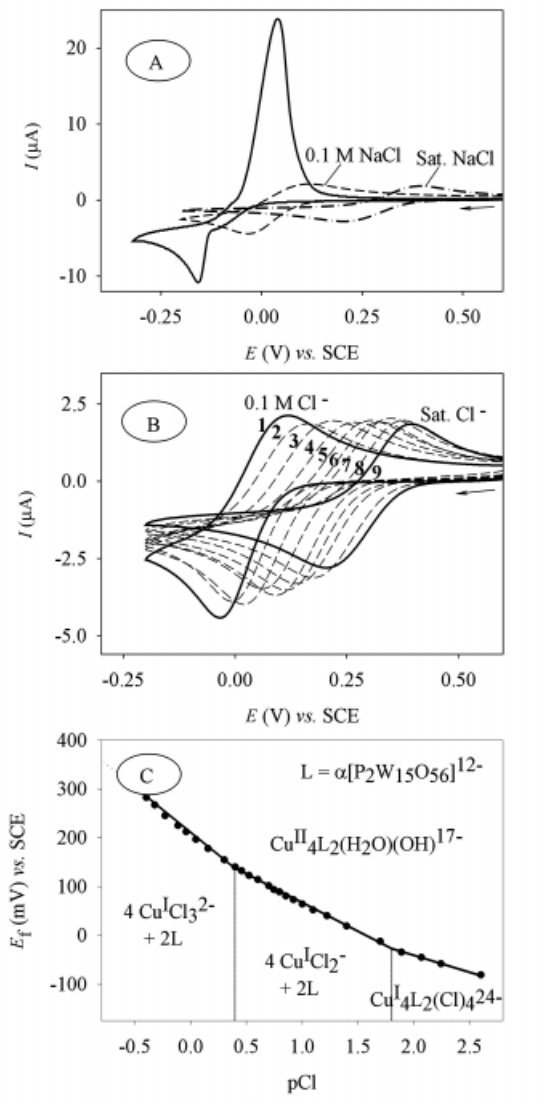

Figure 9. (A) Cyclic voltammograms of 1 mM $Cu_4P_4W_{30}$ in 0.5 M Na_2SO_4 + H_2SO_4 at pH 4.57; scan rate 20 mV s^{-1}; (1) without NaCl (—), (2) in the presence of 0.1 M NaCl (----), and (3) in the presence of saturated NaCl (-.-); (B) evolution of the voltammograms (Cu-centered reduction, Cu^{II}/Cu^{I}) with increasing chloride ion concentration: **1**. 0.1 M NaCl; **2**. 0.2 M NaCl; **3**. 0.4 M NaCl; **4**. 0.8 M NaCl; **5**. 1.2 M NaCl; **6**. 1.6 M NaCl; **7**. 2.0 M NaCl; **8**. 2.8 M NaCl; **9**. saturated solution of NaCl; scan rate 20 mV s^{-1}; pH 4.57; (C) plot of $E_f = (E_{pa} + E_{pc})/2$ vs. pCl (scan rate 20 mV s^{-1}, pH 4.57)

As for $Mn_4P_4W_{30}$, other redox processes can be identified at more positive potentials: at pH 2.52, two reversible one-electron waves are observed at −0.060 V and −0.164 V (ΔE_p = 66 and 68 mV, respectively). Controlled-potential coulometry at −0.245 V in a medium at pH 2.52 and under continuous argon bubbling and stirring consumes 2.10 electrons per molecule, consistent with the reduction of the two Fe^{III} cations.

These waves must thus be attributed to the successive reduction of both Fe^{3+} cations.[12] The couple Fe^{III}/Fe^{II} in $Fe_2P_4W_{30}$ remains fully reversible in the pH range 0.24−7.00, as shown in the inset of Figure 9 and the *E* vs. pH diagram (B in Figure 8). The stability of $Fe_2P_4W_{30}$ was checked by comparison of the CVs obtained immediately after the preparation of the solution and after it had been set aside for at least 4 hours. No variation in current intensities or in the potentials of the different waves was observed; this reproducibility was considered as a sufficient test of the stability of $Fe_2P_4W_{30}$ complexes in these media. The peak currents for the tungsten-based reduction waves and the metal-based reduction waves were seen to vary linearly with the square root of the scan rate up to 500 mV s^{-1} at pH 2.52, which indicates that the electrode reaction is a diffusion-controlled process.

At more acidic pH, i.e. in the pH range 0.24−3.50, Fe-centered redox waves show a negative shift, indicating that they are all accompanied by protonation. It could be shown that the variations in the potentials were of the order of 50−55 mV per pH unit (B in Figure 8), which corresponds to the exchange of one proton.

This result is rather unusual in the case of the Fe-centered redox processes, for which, at low pH, the redox potential is generally almost pH independent.[12c,13]

Assuming that $Fe_2P_4W_{30}$ has the molecular structure recently reported by Hill et al.,[3i,3j] with the two external sites of the sandwich structure occupied by Na^+ cations, the unusual pH dependence can be tentatively explained as follows [Equation (7)−(8)].

At pH < 3.50:

$$[(H_2O)_2Na_2Fe^{III}_2(P_2W_{15}O_{56})_2]^{16-} + e^- + H^+ \leftrightarrows [(H_2ONa)(H_3O)Fe^{III}Fe^{II}(P_2W_{15}O_{56})_2]^{17-} + Na^+ \quad (7)$$

$$[(H_2ONa)(H_3O)Fe^{III}Fe^{II}(P_2W_{15}O_{56})_2]^{17-} + e^- + H^+ \leftrightarrows [(H_3O)_2Fe^{II}_2(P_2W_{15}O_{56})_2]^{18-} + Na^+ \quad (8)$$

$[Cu_4(OH)_2(P_2W_{15}O_{56})_2]^{18-}$ ($Cu_4P_4W_{30}$): Figure 9 shows CVs of 1 mM $Cu_4P_4W_{30}$ at pH 4.57. An irreversible broad peak is observed at −0.15 V, along with an unusual sharp redox anodic peak at about 0.04 V. Similar results have been reported elsewhere for Dawson-type α_2-$P_2W_{17}Cu$ and $ZnW_{11}Cu$.[10]

The sharp anodic peak current increases with the preconditioning time at −0.20 V vs. SCE and with the scan rate. This redox wave is assigned to reduction and oxidation of the transition metal Cu. It is reasonable to expect that both the Cu^{II} and Cu^{I} cations within $Cu_4P_4W_{30}$ will be destabilized by the six-coordinate geometry imposed by the polyoxometallate framework, favoring reduction to Cu^0. In fact, upon reduction, deposition of metallic Cu is observed on the glassy carbon electrode surface, which demonstrates the irreversible dissociation of the complex into α-P_2W_{15}. The anodic peak at 0.04 V should correspond to the reoxidation of Cu^0 to Cu^{2+}. The α-P_2W_{15} anion is not stable in this medium and therefore further decomposition occurs. This accounts for the fact that the W-based waves are irreversible and ill-defined.

Addition of chloride ions to the solution leads to dramatic changes in the electrochemical behavior of $Cu_4P_4W_{30}$, as shown in Figure 9 (B,C). The irreversible cathodic peak at −0.15 V becomes reversible. As this wave, corresponding to copper reduction, is well-separated from the tungsten waves, it is reasonable to assume that this redox process is associated with a $Cu^{II}/Cu^{I}(Cl)_n^{(n-1)}$ couple. The redox potential becomes more negative on increasing the chloride ion concentration. Figure 9 (C) shows a plot of the formal potential vs. pCl. The slopes amount to 64 mV per pCl unit above pCl = 1.8, 121 mV per pCl unit between 1.8 and 0.4, and 177 mV for pCl < 0.4. These results suggest that the Cu-centered reaction mechanism in presence of chloride can be described by Equations (9)−(11).

$$[Cu^{II}_4(H_2O)(OH)(P_2W_{15}O_{56})_2]^{17-} + 4e^- + 4\,Cl^- \leftrightarrows [Cu^{I}_4Cl_4(P_2W_{15}O_{56})_2]^{24-} + OH^- + H_2O\,E_1^{0'}$$
$$[Cu^{I}_4Cl_4(P_2W_{15}O_{56})_2]^{24-} \leftrightarrows 4Cu^{I}Cl(s) + 2\,\alpha\text{-}[P_2W_{15}O_{56}]^{12-} \quad (9)$$

$$[Cu^{II}_4(H_2O)(OH)(P_2W_{15}O_{56})_2]^{17-} + 4e^- + 8\,Cl^- \leftrightarrows 4Cu^{I}Cl_2^- + 2\,\alpha\text{-}[P_2W_{15}O_{56}]^{12-} + OH^- + H_2O\,E_2^{0'} \quad (10)$$

$$[Cu^{II}_4(H_2O)(OH)(P_2W_{15}O_{56})_2]^{17-} + 4e^- + 12\,Cl^- \leftrightarrows 4Cu^{I}Cl_3^{2-} + 2\,\alpha\text{-}[P_2W_{15}O_{56}]^{12-} + OH^- + H_2O\,E_3^{0'} \quad (11)$$

The six-coordinate geometry imposed by the polyoxoanion framework might favor the extraction of the stable $Cu^{I}Cl_n^{(n-1)}$ complex, where n = 1, 2, or 3.

Apparent standard potentials can be calculated from the E_f vs. pCl plot: $E_1^{0'}$ = −0.217 V, $E_2^{0'}$ = −0.109 V, and $E_3^{0'}$ = −0.086 V.

Summary and Concluding Remarks

It is well-known from the literature that the reaction of α-$[P_2W_{15}O_{56}]^{12-}$ with divalent cations M^{2+} leads to sandwich complexes of the general formula $[M_4(H_2O)_2(P_2W_{15}O_{56})_2]^{16-}$ ($M_4P_4W_{30}$). However, in the case of the Fe^{III} and Co^{II} complexes, preparations according to the literature methods, that is in neutral media, invariably give a mixture of several species. In contrast, we have shown that performing the synthesis at low pH leads exclusively to one major isomer with high purity.

The electrochemical behavior of the $M_4P_4W_{30}$ compounds has been investigated systematically at various pH values. All the compounds exhibit three couples due to W-centered reduction processes with slightly different peak potentials from one complex to the next. Two types of sandwich complexes can be distinguished:

(i) For those with Co^{II}, Ni^{II}, Zn^{II}, and Cd^{II}, the metallic centers are electrochemically silent in the potential domains explored in this work.

(ii) For those with Mn^{II}, Fe^{III}, and Cu^{II}, redox reactions originating at the metals M are seen.

The Mn^{II} complex shows an oxidation and two reduction processes, which correspond to oxidation of Mn^{II} to Mn^{IV}, followed, in the reverse scan, by the reduction of Mn^{IV} to Mn^{III} and reduction of Mn^{III} to Mn^{II}. The compound $Cu_4P_4W_{30}$ exhibits a deposition process accompanied by decomposition of the copper complex. Extraction of the copper(I) complexes $Cu^{I}Cl_n^{(n-1)}$ (n = 1−3) can also be observed upon reduction of the polyoxoanions in the presence of chloride ions.

Finally, the compounds $[Fe_4(H_2O)_2(P_2W_{15}O_{56})_2]^{12-}$ and $[(H_2O)_2Na_2Fe_2(P_2W_{15}O_{56})_2]^{16-}$ both exhibit Fe-centered redox processes prior to reductions of the polyanions. Splitting of this wave often occurs.

This series of sandwich polyoxoanion complexes would appear to be quite promising in relation to electrocatalytic reactions; in particular, the Mn^{II} sandwich complex is a potential candidate for both oxidative and reductive catalysis. $[(H_2O)_2Na_2Fe_2(P_2W_{15}O_{56})_2]^{16-}$ also appears to be quite promising and may find application in the preparation of pure mixed sandwich complexes of the type $[M^{II}_2Fe^{III}_2(H_2O)_2(P_2W_{15}O_{56})_2]^{14-}$.

Electrocatalytic processes of this type, both in aqueous solution and in organic media, and the preparation of new $[M^{II}_2Fe^{III}_2(H_2O)_2(P_2W_{15}O_{56})_2]^{14-}$ complexes are currently under investigation.

Experimental Section

General: Most common laboratory chemicals were reagent grade, as purchased from commercial sources, and were used without further purification.

Preparation of the Compounds: The potassium salt of α-$[P_2W_{18}O_{62}]^{6-}$ and the sodium salt of α-$[P_2W_{15}O_{56}]^{12-}$ were prepared by published methods.[2] An extensive series of tetranuclear divalent Dawson-derived sandwich complexes of the formula $[M_4(H_2O)_2(P_2W_{15}O_{56})_2]^{16-}$ (where M = Mn^{II}, Ni^{II}, Zn^{II}, Cd^{II}) were prepared as described elsewhere.[3] All samples were recrystallized as described in the original procedures and were characterized by IR spectroscopy and ^{31}P NMR spectrometry.

$Na_{16}[(H_2O)_2Na_2Fe_2(P_2W_{15}O_{56})_2]\cdot 53H_2O\cdot 4NaCl$: $FeCl_3\cdot 6H_2O$ (0.34 g, 1.25 mmol) was dissolved in 1 M aq. NaCl/0.1 M aq. HCl (pH 1) (50 mL) with stirring. α-$Na_{12}P_2W_{15}O_{56}\cdot 24H_2O$ (5.00 g, 1.13 mmol) was then added under vigorous stirring. The solution was heated at 80 °C until the volume had been reduced to ca. 12.5 mL. It was then filtered hot and the filtrate was left to stand in air. After evaporation of the solvent, 1 M aq. NaCl (5 mL) was added with stirring. A yellow solid was precipitated, which was collected by filtration and dried in air; yield 3.49 g (0.38 mmol; 67%). $Cl_4Fe_2Na_{22}O_{112}P_4W_{30}\cdot 55H_2O$: calcd. Fe 1.22, P 1.35, W 60.08, H_2O 10.79; found Fe 1.24, P 1.35, W 59.89, H_2O 10.76.

The purity of the compound was checked by ^{31}P NMR in D_2O, which showed a single resonance [P(2)] at δ = −11.2 ($\Delta\nu_{1/2}$ = 220 Hz). The signal of the phosphorus atom nearest to the paramagnetic Fe^{III} ions [P(1)] was not observed.

$Na_{11}H[Fe^{III}_4(H_2O)_2(P_2W_{15}O_{56})_2]\cdot 45H_2O$: This complex was prepared as follows by a modification of the literature method:[3i] $FeCl_3\cdot 6H_2O$ (0.82 g, 3.01 mmol) was dissolved in 1 M NaCl/0.1 M HCl (pH ≈ 1) (40 mL) with stirring. α-$Na_{12}P_2W_{15}O_{56}\cdot 24H_2O$ (6.00 g, 1.36 mmol) was then slowly added under vigorous stirring. The solution was heated at 80 °C until the volume had been reduced to ca. 12.5 mL. It was then filtered hot and the filtrate was left to stand in air. After evaporation of the solvent, 1 M aq. NaCl (5 mL) was added with stirring. A yellow solid precipitated, which was collected by filtration, dried in air, and recrystallized from 2 M aq. NaCl; yield: 3.09 g (0.35 mmol; 52%). $Fe_4Na_{11}HO_{112}P_4W_{30}\cdot 47H_2O$: calcd. Fe 2.55, P 1.41, W 63.00, H_2O 9.67; found Fe 2.69, P 1.38, W 62.98, H_2O 9.78.

The purity of the compound was checked by ^{31}P NMR, which showed two resonances at δ = −11.7 [P(2); $\Delta\nu_{1/2}$ = 55 Hz] and δ = +915 [P(1); $\Delta\nu_{1/2}$ = 2500 Hz].

$Na_{17}[Co_4(H_2O)(OH)(P_2W_{15}O_{56})_2]\cdot 51H_2O\cdot 2NaCl$: $Co(NO_3)_2\cdot 6H_2O$ (0.73 g, 2.25 mmol) was dissolved in 1 M aq. NaCl/0.1 M aq. HCl (50 mL) with stirring. α-$Na_{12}P_2W_{15}O_{56}\cdot 24H_2O$ (5.00 g, 1.13 mmol) was then slowly added under vigorous stirring. The solution was heated at 40 °C for 15 min (pH 3), then filtered hot and the filtrate was left to stand in air. After evaporation of the solvent, 1 M aq. NaCl (5 mL) was added with stirring. A pale green-brown solid was precipitated, which was collected by filtration and dried in air; yield 3.99 g (0.44 mmol, 78%). $Cl_2Co_4Na_{18}P_4W_{30}O_{112}\cdot OH\cdot 52H_2O$: calcd. Co 2.59, P 1.35, W 60.34, H_2O 10.87; found Co 2.77, P 1.30, W 60.10, H_2O 11.16.

The purity of the compound was checked by ^{31}P NMR, which showed two resonances at δ = 9.9 [P(2); $\Delta\nu_{1/2}$ = 20 Hz] and δ = 1483 [P(1); $\Delta\nu_{1/2}$ = 420 Hz].

$Na_{16}Cu[Cu_4(OH)_2(P_2W_{15}O_{56})_2]\cdot 53H_2O$: This complex was prepared, as follows, by a method slightly different from that reported elsewhere:[3c] $CuCl_2$ (0.35 g, 2.50 mmol) was dissolved in 1 M aq. NaCl (50 mL) with stirring. α-$Na_{12}P_2W_{15}O_{56}\cdot 24H_2O$ (5.00 g, 1.13 mmol) was then slowly added under vigorous stirring. The solution was heated at 40 °C until the P_2W_{15} had completely dissolved. It was then filtered hot and the filtrate was left to stand in air for one day at room temperature and then cooled to 5 °C. Pale-green crystals were deposited after two days, which were collected by filtration and dried in air; yield (3.20 g, 0.35 mmol, 62%). $Cu_5Na_{12}O_{112}P_4W_{30}\cdot 2(OH)\cdot 53H_2O$: calcd. Cu 3.52, P 1.37, W 60.87, H_2O 10.58; found Cu 3.43, P 1.37, W 60.88, H_2O 10.26.

The purity of the compound was checked by ^{31}P NMR, which showed a single resonance at δ = −16.2 ($\Delta\nu_{1/2}$ = 60 Hz). This line was assigned to P(2), the more distant P atom from the Cu^{II} center. The signal from the phosphorus atom designated P(1) nearest to the paramagnetic Cu^{II} ions was not observed.

NMR, IR, and Potentiometric Measurements: ^{31}P NMR spectra were recorded from sample solutions in 5 mm o.d. tubes on a Bruker AC 300 spectrometer operating at 121.5 MHz in Fourier-transform mode (equipped with a QNP probe for ^{31}P NMR). The ^{31}P chemical shifts were measured at 300 K using 0.02 M solutions of the polyanions in 0.5 M aqueous LiCl (50% D_2O) solutions and were referenced to external 85% H_3PO_4 (IUPAC convention) by the substitution method.

IR spectra were recorded on a Bio-Rad FTS 165 FTIR spectrophotometer from samples in KBr pellets.

Potentiometric measurements were made on a Tacussel PHN330T pH meter. Constant ionic strength (μ = 0.1 M, $NaNO_3$) was used in the titrations. In potentiometric titrations, the dilution was less than 2%.

Electrochemical Experiments

Chemicals, Equipment, and Apparatus: Pure water was used throughout. It was obtained by passing water through a Milli-RO_4 unit and subsequently through a Millipore Q water purification set. H_2SO_4 and Na_2SO_4 were commercial products (Prolabo). The pH 2 electrolyte was made up from 0.5 M Na_2SO_4 and the pH was adjusted by the addition of 0.5 M (H_2SO_4 + Na_2SO_4). Other pHs were obtained by the addition of H_2SO_4 or NaOH (Prolabo) as appropriate. The solutions were thoroughly deaerated for at least 30 min by bubbling pure argon and were kept under argon pressure during the experiments.

The source, mounting, and polishing of glassy carbon (GC, Tokai, Japan) have been described previously.[14] The glassy carbon samples for use as electrodes had a diameter of 3 mm. The electrochemical set-up consisted of an EG&G 273 A potentiostat driven by a personal computer with 270 software. Potentials are quoted with respect to a saturated calomel electrode (SCE). The counter-electrode was a platinum gauze of large surface area. All voltammetric experiments were carried out at room temperature.

Analyses: Elemental analyses were performed by classical gravimetric, potentiometric, and spectrophotometric methods.

The anions were first decomposed in boiling concentrated hydrochloric acid solution. Tungsten and phosphorus were then precipitated together by adding cinchonium hydrochloride. They were determined simultaneously as WO_3 and P_2O_5 by gravimetry after calcination of the cinchonium salt. Cobalt, which remained in the filtrate, was complexed with ammonia and then titrated as hexacyanocobaltate(III) complex by potentiometry. Phosphorus was determined by spectroscopy of the molybdovanadophosphate.[15] Water content was determined by thermogravimetric analysis. The other metallic elements (Fe, Cu) were analyzed by atomic absorption spectroscopy.

Supporting Information (see footnote on the first page of this article): Comparison of the IR spectra (KBr) of the hydrated sandwich heteropolyanion series.

Acknowledgments

This work was supported by the CNRS and by the Universities Paris XI and Paris VI. We are also grateful to Martine Richet for performing the microanalyses.

[1] [1a] B. Keita, L. Nadjo, R. Contant, M. Fournier, G. Hervé, French Patent (CNRS) 8911, 728; February 10, **1989**. [1b] B. Keita, L. Nadjo, R. Contant, M. Fournier, G. Hervé, Eu. Patent (CNRS), Appl. EP 382,644; *Chem. Abstr.* **1991**, *114*, 191882u. [1c] B. Keita, A. Belhouari, L. Nadjo, R. Contant, *J. Electroanal. Chem.* **1995**, *181*, 243−250. [1d] M. Abbessi, R. Contant, R. Thouvenot, G. Hervé, *Inorg. Chem.* **1991**, *30*, 1695−1702. [1e] B. Keita, K. Eassadi, L. Nadjo, R. Contant, Y. Justun, *J. Electroanal. Chem.* **1996**, *404*, 271−279. [1f] J. F. Garvey, M. T. Pope, *Inorg. Chem.* **1978**, *17*, 1115−1118. [1g] B. Keita, Y. W. Lu, L. Nadjo, R. Contant, M. Abbessi, J. Canny, M. Richet, *J. Electroanal. Chem.* **1999**, *477*, 146−157.

[2] [2a] J.-P. Ciabrini, R. Contant, J.-M. Fruchart, *Polyhedron* **1983**, *2*, 1229−1233. [2b] R. Contant, J.-P. Ciabrini, *J. Chem. Res.* **1977**, (S) 222, (M) 2601−2609. [2c]R. Contant, *Inorg. Synth.* **1990**, *27*, 104−109.

[3] [3a] R. G. Finke, M. W. Droege, *Inorg. Chem.* **1983**, *22*, 1006−1008. [3b] R. G. Finke, M. W. Droege, P. J. Domaille, *Inorg. Chem.* **1987**, *26*, 3886−3896. [3c] T. J. R. Weakley, R. G. Finke, *Inorg. Chem.* **1990**, *29*, 1235−1241. [3d] J.-P. Ciabrini, R. Contant, *J. Chem. Res.* **1993**, *(S) 391*, (M) 2719−2744. [3e] C. J. Gómez-García, J. J. Borrás-Almenar, E. Coronado, L. Ouahab, *Inorg. Chem.* **1994**, *33*, 4016−4022. [3f] R. G. Finke, T. J. R. Weakley, *J. Chem. Cryst.* **1994**, *24*, 123−128. [3g] J. F. Kirby, L. C. W. Baker, *J. Am. Chem. Soc.* **1995**, *117*, 10010−10016. [3h] N. J. Crano, R. C. Chambers, V. M. Lunch, M. A. Fox, *J. Mol. Cat. A: Chem.* **1996**, *114*, 65−75. [3i] X. Zhang, D. C. Duncan, C. F. Campana, C. L. Hill, *Inorg. Chem.* **1997**, *36*, 4208−4215. [3j] X. Zhang, T. M. Anderson, Q. Chen, C. L. Hill, *Inorg. Chem.* **2001**, *40*, 418−419. [3k] A. Müller, F. Peter, M. Pope, D. Gatteschi, *Chem. Rev.* **1998**, *98*, 239−271. [3l] L. Meng, J. F. Liu, *Chem. Res. in Chinese Universities* **1998**, *14*, 1−5. [3m] X. Zhang, C. L. Hill, *Chem. Ind.* **1998**, *75*, 519−524.

[4] [4a] L. C. W. Baker, *Plenary Lecture, Proc. XV Int. Conf. Coord. Chem. 15th*, Moscow, **1973**. [4b] D. K. Lyon, W. K. Miller, T. Novet, P. J. Domaille, E. Evitt, D. C. Johnson, R. G. Finke, *J. Am. Chem. Soc.* **1991**, *113*, 7209−7221.

[5] R. Contant, M. Abbessi, J. Canny, A. Belhouari, B. Keita, L. Nadjo, *Inorg. Chem.* **1997**, *36*, 4961−4967.

[6] C. Rocchiccioli-Deltcheff, R. Thouvenot, R. Franck, *Spectrochim. Acta* **1976**, *22A*, 587−597.

[7] C. Rocchiccioli-Deltcheff, R. Thouvenot, *J. Chem. Res.* **1977**, (S) *46−47*, (M) 549−571.

[8] C. Rocchiccioli-Deltcheff, R. Thouvenot, *Spectrosc. Lett.* **1979**, *12*, 127−138.

[9] T. L. Jorris, M. Kozik, N. Casañ-Pastor, P. J. Domaille, R. G. Finke, W. K. Miller, L. C. W. Baker, *J. Am. Chem. Soc.* **1987**, *109*, 7402−7408.

[10] [10a] L. Cheng, H. Seen, J. Liu, S. Dong, *J. Chem. Soc., Dalton Trans.* **1999**, 2619−2625. [10b] B. Keita, E. Abdeljalil, L. Nadjo, B. Avisse, R. Contant, J. Canny, M. Richet, *Electrochem. Commun.* **2000**, *2*, 145−149.

[11] [11a] D. E. Katsoulis, M. T. Pope, *J. Chem. Soc., Dalton Trans.* **1989**, 1483−1489. [11b] C. L. Hill, R. B. Brown, *J. Am. Chem. Soc.* **1986**, *108*, 536−538. [11c] D. Mansuy, J. F. Bartoli, D. K. Lyon, R. C. Finke, *J. Am. Chem. Soc.* **1991**, *113*, 7222−7226. [11d] C. M. Tourné, G. F. Tourné, S. M. Malik, T. J. R. Weakley, *J. Inorg. Nucl. Chem.* **1970**, *32*, 3875−3890. [11e] X. Y. Zhang, M. T. Pope, M. R. Chance, G. B. Jameson, *Polyhedron* **1995**, *14*, 1381−1392. [11f] X. Y. Zhang, G. B. Jameson, C. J. O'Connor, M. T. Pope, *Polyhedron* **1996**, *15*, 917−922. [11g] X. Y. Zhang, C. J. O'Connor, G. B. Jameson, M. T. Pope, *Inorg. Chem.* **1996**, *35*, 30−34. [11h] M. Sadakane, E. Steckhan, *J. Mol. Catal. A.* **1996**, *114*, 221−228. [11i] A. Muller, L. Dloczik, E. Diemann, M. T. Pope, *Inorg. Chim. Acta* **1997**, *257*, 231.

[12] [12a] S. Dong, M. J. Liu, *J. Electroanal. Chem.* **1994**, *372*, 95−100. [12b] B. Fabre, G. Bidan, M. Lapkowski, *J. Chem. Soc., Faraday Trans.* **1997**, 591−601. [12c] T. McCormac, B. Fabre, G. Bidan, *J. Electroanal. Chem. Interfacial Electrochem.* **1997**, *425*, 49−54. [12d] T. McCormac, B. Fabre, G. Bidan, *J. Electroanal. Chem. Interfacial Electrochem.* **1997**, *427*, 155−159. [12e] J. E. Toth, F. C. Anson, *J. Electroanal. Chem. Interfacial Electrochem.* **1988**, *256*, 361−370. [12f] J. E. Toth, F. C. Anson, *J. Am. Chem. Soc.* **1989**, *111*, 2444−2451. [12g] J. E. Toth, J. D. Melton, D. Cabelli, B. H. J. Bielski, F. C. Anson, *Inorg. Chem.* **1990**, *29*, 1952−1957. [12h] K. K. Shiu, F. C. Anson, *J. Electroanal. Chem. Interfacial Electrochem.* **1991**, *309*, 115−119.

[13] B. Keita, A. Belhouari, L. Nadjo, R. Contant, *J. Electroanal. Chem.* **1998**, *442*, 49−57.

[14] B. Keita, K. Essaadi, L. Nadjo, *J. Electroanal. Chem. Interfacial. Electrochem.* **1989**, *259*, 127−146.

[15] B. Cherreton, F. Chauveau, G. Bertho, P. Courtin, *Chim. Anal.* **1965**, *47*, 17.

Received August 13, 2001
[I01305]